This may be the author's version of a work that was submitted/accepted for publication in the following source:

A vision-based sense-and-avoid system tested on a ScanEagle UAV

Dmitry Bratanov, Luis Mejias and Jason J. Ford.

Abstract—This paper presents a study of near collision course engagements between a Cessna 172R aircraft and a ScanEagle UAV carrying a custom built vision-based sense-and-avoid system. Vision-based systems are an attractive solution for the sense-and-avoid problem because of size, weight and power considerations. We present post flight test analysis that shows our detection system successfully detecting an approaching Cessna aircraft in all 15 flight test encounters at ranges greater than 1500 m, with no false alarms events. Moreover, this paper characterises the image inter-frame stabilisation required to achieve acceptable detection performance, and compares a range of stabilisation techniques for achieving this type of stabilisation precision. Our analysis illustrates that the image inter-frame stabilisation requirements are demanding, suggesting that images must be stabilised in real-time at 9Hz to within 2 pixels between consecutive frames. We present performance comparisons between stabilisation using GPS/INS, IMU-only and image-based techniques.

I. INTRODUCTION

The current limitation of small-to-medium sized unmanned aerial vehicles (UAVs) to replicate onboard human pilot ability to sense-and-avoid (SAA) other aircraft, is one of the main obstacles to greater integration of UAVs into national airspace, and the routine and regular use of UAV for commercial and civil applications in non-segregated airspace [1], [2], [3], [4], [5]. A key challenge within the SAA problem is to reliably and automatically detect potential mid-air aircraft collisions (due to cost, power, size and weight limitations that exclude well proven technology such as radar for small to mediums sizes UAVs)[4]. Recently, vision-based aircraft detection approaches have been shown to provide a candidate approach for automated onboard mid-air aircraft collision detection [6], [7], [8] (at least for detection from sky-region backgrounds, under moderate to good lighting conditions). However, these initial solutions have required high accuracy inertial navigation systems (INS) to provide an appropriate level of image stabilisation [6]. This image stabilisation issue is examined in detail in this paper, and several (low cost) approaches are characterised.

An automated vision-based SAA system would need to detect any potential collision threats at sufficient distances to allow enough time to avoid any potential collisions (typically greater than 1 km) [9]. At these distances, at the angular resolutions provided by current technologies, any potential collision aircraft will only occupy a small number of image pixels [9]. Over the last few decades, multi-stage morphological-temporal filtering approaches have emerged

as the leading candidates for achieving vision-based aircraft collision detection (from sky-region backgrounds)[6], [7], [8], [10], [11], [12]. These approaches required that the any apparent image motion has been compensated using an appropriate image stabilisation process (which has been achieved in past studies through the use of expensive tactical grade integrated GPS/INS system [7]).

The first contribution of this paper is the evaluation of a custom built vision-based sense-and-avoid system fitted to a ScanEagle UAV that is capable of reliable low-false alarm sky-region aircraft collision detection. Motivated by the importance and current cost of achieving inter-frame stabilisation, a second contribution of this paper is to characterise the inter-frame stabilisation requirement in terms of overall system performance. This leads to a statement of the stabilisation requirement in terms of the allowable residue inter-frame motion remaining after the stabilisation process. The final contribution of this paper is an examination of several competing technologies for achieving stabilisation, which shows that the stabilisation requirement can be achieved by an IMU-only based approaches that has lower cost than a tactical grade GPS/INS approach.

This paper is structured as follows: In Section II, we briefly provide an overview of the vision-based detection system fitted to a ScanEagle UAV for testing purposes. In Section III, we describe several candidate stabilisation techniques. In Section IV, we present stabilisation analysis studies, before presenting conclusions in Section V.

II. AN AUTOMATED VISION-BASED AIRCRAFT DETECTION SYSTEM FOR UAVS

Over the last few years, spatial-temporal filter detection approaches have emerged as candidate vision-based aircraft detection systems for the SAA problem (at least for detection of aircraft collisions emerging from the sky-region), for instance see the approaches in [7], [8], [13]. However, a SAA system will likely have a high degree of customisation due to the different requirements and operational contexts of each UAV. For a detailed overview of current technologies and contexts, the reader is referred to [14], [15] (and references within). For sky-region collision detection, our system involve the components shown in Figure 1. In this section, we briefly describe each of the components of this custom built vision-based SAA system that has been fitted to a ScanEagle UAV as shown in Figure 2.

Physical mount: The detection system needs to be physically mounted on the platform to allow sensing in the direction of potential collision course aircraft. In addition to allowing sensing in the desired direction, the mounting

School of Electrical Engineering and Computer Science Queensland University of Technology. Brisbane, Australia 4001. {dmitry.bratanov, luis.mejias, j2.ford}@qut.edu.au
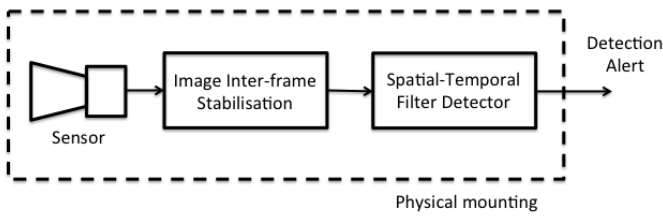
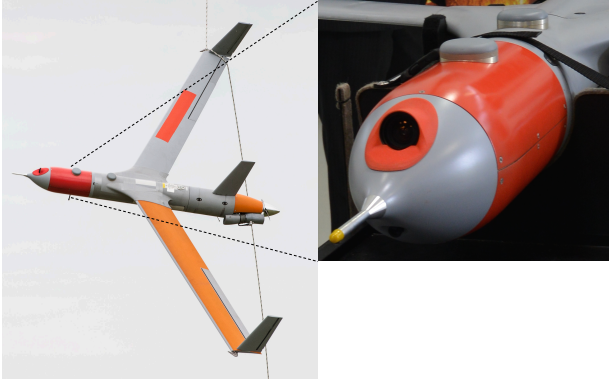Fig. 1. The basic components of a spatial-temporal filter detection system.

Fig. 2. Captured ScanEagle carrying a custom built nose mounted detection system (left). Details of the custom built nose mounted detection system (right). Note the detection system contains its own GPS/INS independent of the host UAV.

system should protect the sensor, and provide a low vibration sensing environment. Past examples of physical mounting approaches include: mounting above the airframe [6], mounting on a wing strut [7], or mounting on the nose of the platform [9], [16]. In the developed system, as shown in Figure 2, the detection system was mounted on the nose of the ScanEagle UAV for the purposes of real-time detection of an approaching aircraft.

Sensor: A visual sensor and optical lens combination needs to be selected to visually sense potential collision course aircraft at sufficient ranges with reasonable field-of-view (FOV). Past sensing systems include: 1024×768 pixel Basler Scout Series camera [6], [7] and a 8 Mega pixel sensor [16]. Also a range of sensors and FOV choices were examined in [8], [12]. In addition, the suitability of infrared sensors for this application was examined in [17] and conformal sensors of different types in [18]. With current technology, a single sensor is unlikely to achieve the FOV requirements, but several researchers have suggested mounting configurations involving multiple sensors [9], [16], [19].

The developed system used a commercial off the shelf (COTS) Point Grey Grasshopper 50S5M-C 5MP (mono) camera with a 5mm focal length lens Navitar NMV-5m-23. As an initial prototype, our detection system uses a single sensor that achieves a suitable detection range but with smaller FOV than might be desired (such as suggested in [1], [9]), with the understanding that a future system could be developed on the basis of multiple sensors. This sensor

is body-mounted in a forward looking direction (i.e. not gimbal mounted). Although this camera has a high resolution capability, for computational reasons only a centred region of interest (ROI) of 1024×768 pixels (corresponding to a FOV of $41.5° \times 28.7°$) was processed at 9Hz (mono 8-bit).

Spatial temporal filter detector: This is the key component of a sky-region aircraft collision detection system that performs image processing to produce a detection alert. Past approaches include: morphological-dynamic programming approaches [7], [11], [20], Morphological-Hidden Markov model filtering approaches [6], [7], [20], Morphological-Extended Kalman filter approaches [16], [18], [21]. Some approaches have also used shape descriptions, SVM-based classification [8], [21] or feature detection techniques [22].

These spatial temporal filter detector algorithms can be implemented in real-time using specialised computational hardware. Details of past Morphological-Hidden Markov model filtering implementations on specialised Graphic Processing units (GPUs) are provided in [13], [23]. Examples of FPGA implementations of other SAA detection approaches are given in [3], [9], [19].

The developed system used a Morphological-Hidden Markov model filtering approach, which is extensively described in [7] and references within. In this implementation we used the filter described in [7], except for the 3×3 morphological structuring element. We highlight that this filter has been designed to allow a maximum of 2 pixels motion of the target between frames (see [6], [7] for justification on this value, this 2 pixels motion number will play an important role in our later analysis studies). The algorithm was implemented on a NVIDIA GeForce 9400M GPU with 16 graphical cores which allowed image processing at 9Hz.

Detection alert: A detection alert is produced by the spatial temporal filter detector and is available for use by other systems on the UAV. For example, it could be used to trigger a collision avoidance action as described in [24], [25], [26]. In particular, the Morphological-Hidden Markov model filtering approach used in the developed system produce a detection statistic η_k. A threshold T_D was selected, and a detection alert issued whenever $\eta_k > T_D$.

Image inter-frame stabilisation: An image inter-frame stabilisation stage is required to minimise the inter-frame motion between image frames, so that there are suitable measurements for the spatial-temporal filter detection approach [6], [17]. In particular, the requirement for inter-frame stabilisation stems from the temporal filtering stage of the detection approach which requires that there is a correspondence between the pixel locations in successive frames.

The developed system contained a GPS/INS NovAtel ADIS-SPAN system with custom built image capture synchronisation to facilitate image stabilisation (that is, within the custom built nose section, and not dependent on the ScanEagle UAV). The primary focus of this paper is to investigate and characterise the image inter-frame stabilisation component of the developed system, and this stabilisation technology will be described in more detail in the following

section.

III. IMAGE INTER-FRAME STABILISATION TECHNOLOGIES

One of the important outcomes of this paper is the characterisation and study of inter-frame stabilisation approaches in terms of overall system performance. There have been two main approaches for inter-frame stabilisation suggested in the context of the sky-region vision-based aircraft detection problem: inertial measurement based stabilisation [7], [16], and image-based stabilisation [6]. In this section, we describe several candidate stabilisation approaches before we proceed to examine their effects on the overall detection system performance in Section IV.

A. Aircraft GPS/INS attitude based image inter-frame motion stabilisation

In the previous studies [7], a high accuracy onboard GPS/INS system was used to estimate aircraft heading, pitch and roll angles. In the following, we will describe a method for using this high-quality aircraft attitude information (heading, pitch and roll angles) to compensate for inter-frame image motion (an alternative approach is described in [17]).

Let ϕ_k, θ_k, ψ_k denote the sensed roll, pitch and heading (or yaw) angles of the aircraft at time $k > 0$ (for example, sensed by our GPS/INS NovAtel ADIS-SPAN system). First, let us smooth the heading angle to allow for yawing motion of the aircraft in the following manner:

$$\psi_k^{MA} = (1 - \alpha)\psi_{k-1}^{MA} + \alpha\psi_k \tag{1}$$

where $\alpha = 0.01$ has experimentally been found to be a reasonable smoothing coefficient, and the smoothed angle is initialised so that $\psi_0^{MA} = \psi_1$. Then the image is roll compensated using Nvidia's built in roll compensation function of ϕ_k available on our GPU hardware which also implements translation compensation by calculated amounts

$$\begin{aligned}
\Delta x_k &= f_x \tan(\theta_k - \theta^*) \\
\Delta y_k &= f_y \tan(\psi_k - \psi_k^{MA})
\end{aligned} \tag{2}$$

where θ^* is camera mounting offset angle, $f_x = 1408$ pixels and $f_y = 1405$ pixels are the calibrated focal lengths of our camera system in the x and y directions.

B. Aircraft IMU-only based image inter-frame stabilisation

The detection system is sensitive to inter-frame motion, rather than accuracy of the attitude information. This observation motivates consideration of estimating inter-frame motion directly from inertial measurement unit (IMU) information (with the benefit of avoiding an expensive GPS/INS sensor). Low computational load and ability to operate at small sampling rates significantly reduces power and hardware necessary for image stabilisation in target detection.

One recently proposed IMU-only attitude estimation approach is the IMU based gradient descent orientation algorithm [27] that estimates heading $\hat{\psi}_k$, pitch $\hat{\theta}_k$, roll $\hat{\phi}_k$ angles with minimal drift. We applied this gradient descent algorithm (which adjustable drift parameter set at $b = 0.01$)

to the raw 200 Hz Analog Devices ADIS-16488 IMU sensor data (part of the NovAtel ADIS-SPAN system). The algorithm's estimated quaternions were used to construct Euler angle estimates $\hat{\phi}_k$, $\hat{\theta}_k$, $\hat{\psi}_k$ in the standard manner.

Comparison with a custom built unscented Kalman filter-based approach for IMU-only attitude estimation (and fully GPS/INS attitude solution) confirmed the observations in [27] that this gradient descent algorithm performs no worse as conventional Kalman filter-based IMU-only attitude estimation techniques, whilst avoiding the usual parameter tuning burdens. Once an attitude estimate is produced, it can be mechanised into roll and lateral shifts of the image by using (1)-(2) but with $\hat{\phi}_k$, $\hat{\theta}_k$, $\hat{\psi}_k$ used in place of ϕ_k, θ_k, ψ_k, respectively.

C. Image-based stabilisation technologies

Image-based stabilisation is performed by first estimating motion of the camera by analysing successive frames in a video sequence. The motion of the camera is usually described by a 3D dimensional motion vector, however for stabilisation purposes only motion in 2D is generally used. Once motion is estimated, the image is then shifted by an amount proportional to the motion vector. There are two main categories when describing motion estimation techniques: feature-based and intensity-based. Feature-based methods establish a correspondence between pairs of selected feature points in two frames, and then attempts to match them together in a motion model. This is more often useful for applications of motion tracking. Intensity-based methods rely on a constant intensity assumption, whereby the apparent motion can be computed by measuring variations of intensity values over time. This resulting pattern is a vector field known as the optical flow field. In this paper, we make use of feature-based techniques, and in particular, the Lucas-Kanade method to estimate optical flow [28]. This is a well established technique with many implementations, here we used OpenCV version [29]. For details on this technique refer to [30] and references within. Once optic flow is estimated, a standard homography is applied to find the camera angles between two consecutive frames. Finally, the current image is stabilised (shifted) using the pitch and roll angles previously estimated.

IV. FLIGHT TESTS AND DETECTION PERFORMANCE STUDIES

In this section we conduct analysis studies related to the image stabilisation process. We begin this section by the describing the flight test data captured with the payload fitted to a ScanEagle UAV [31]. Then, on the basis of this flight test, we examine the baseline performance of the system when using the GPS/INS NovAtel ADIS-SPAN attitude solution for inter-frame image stabilisation. We then examine the impact of inter-frame motion on the detection performance by adding increasing levels of artificial inter-frame image motion and then observing the resulting detection distance performance of the system. This study leads to a description of the image stabilisation requirement to

Fig. 3. Different environment conditions from the flight test datasets (zoomed to 450x500 pixel) in Encounter 2.

Fig. 4. Effect of the rain drop in three consecutive frames: no drop on the left image, circular shaped drop contacted the lens in the centre, drop disappearing due to airflow on the right image. Encounter 15.

ensure reliable detection. Finally, we conduct a comparison study of various stabilisation approaches to evaluate a range of proposed image stabilisation techniques.

A. Data capture

Data was captured from 15 head-on near collision course encounters between a ScanEagle UAV carrying the custom-built detection system and a Cessna 172R aircraft using the approach described in [7]. During these flight tests, encounters 1-5 were conducted in the afternoon with good visibility, encounters 6-13 were conducted in the morning with hazy visibility due to approaching inclement weather, and encounters 14-15 were conducted in light rain conditions. Figure 3 shows an example of sun reflections (frame 35, 1st encounter) and aircraft looking alike cloud features (frame 687, 2nd encounter). Figure 4 shows 450x500 pixel zoomed fragments of collected consecutive frames during large rain drop and lens contact in 15th encounter. An illustrative sample frame from encounter 14 is shown in Figures 5 and 6.

B. Baseline system performance

Baseline stabilisation (GPS/INS image stabilisation): The captured image sequences were stabilised using the GPS/INS approach described in Section III-A. Detailed manual analysis of these stabilised image sequences showed that much of the raw inter-frame image motion had been removed but that some residue of uncompensated inter-frame motion remained (this is not completely surprising due to the attitude accuracy limits of such inertial systems). Four of the 15 GPS/INS compensated image sequences (encounters 1, 8, 12 and 13, or 1046 frames in total) were manually analysed, and the observed feature motion between frames was used

Fig. 5. Illustrative image frame from encounter 14 just after target is detected (frame 790). The black region at bottom of the image is a result of image stabilisation. The location of the detected target is shown by the black box.
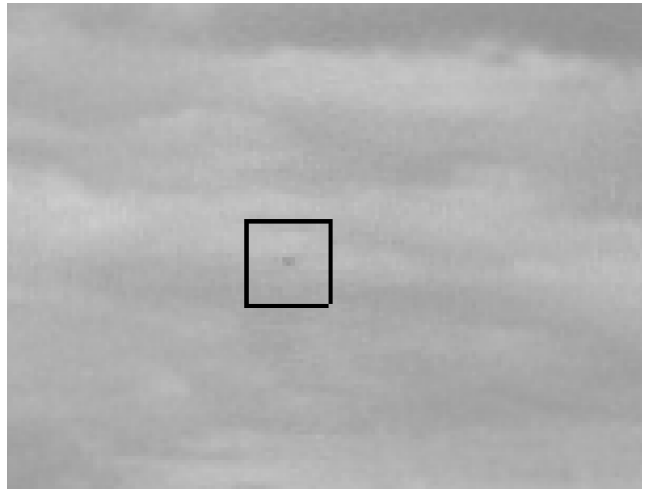

Fig. 6. Illustrative image frame cropped to show target (cropped from image frame shown in Figure 5). The aircraft is at a distance of 1900 metres.

to estimate the amount of residue (or uncompensated) inter-frame motion, which was 1.1 pixels per frame with a standard deviation of 0.74 pixels.

Baseline detection performance: We now examine the detection performance of the baseline system when using an GPS/INS image stabilisation approach. Figure 7 illustrates the typical behaviour of the baseline system's detection statistic (noting that higher values represent higher probabilities that a target is present). As shown in this figure, during a (near) collision course encounter the range between aircraft will decrease until the aircraft are close enough and the detection metric starts to rise. The strong distinct increase in detection statistic between distances of 2000 m to 1000 m suggests that it is possible to achieve high probability of detection with low probability of false alarm by appropriately setting the threshold value T_D.

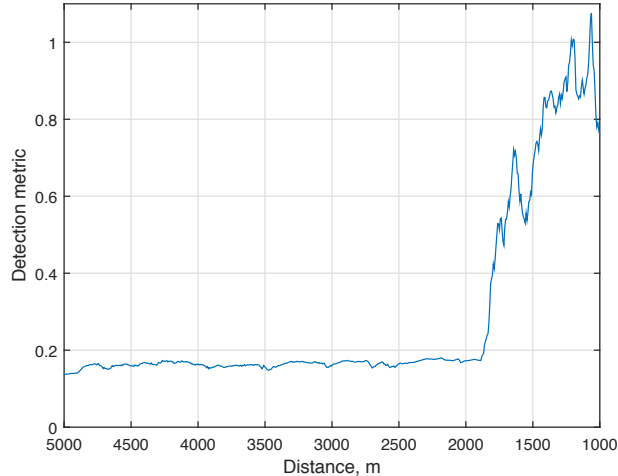Under a more detailed evaluation of all encounters, the

Fig. 7. Example of detection metric η_k versus range (13th encounter). Once aircraft is within a certain range, the detection metric is very distinct.

Threshold T_D	0.45	0.6	0.8
Range	$1886(156.9)\ m$	$1805(149.1)\ m$	$1606(129.7)\ m$

baseline system with a detection threshold of 0.45 or above successfully detected the near collision aircraft in all 15 encounters, with no false alarms. Table I shows a comparison of average detection range achieved for different threshold choices. This study illustrates that the baseline system robustly detected near collision course targets in this experimental data set, and moreover illustrated that lower threshold value can potentially achieve earlier detection (or equivalently detection at longer range), but admittedly with the potential of increased risk of false alarm events.

Hence the baseline system with GPS/INS image stabilisation approach seems to provide a credible technological approach towards an automated image SAA technology for UAVs. Two questions that arise are whether the high quality stabilisation offered by the (high cost) GPS/INS technology is actually required, and whether a cheaper or lighter technological solution might be adequate. We will study these two questions in the following analysis.

C. Evaluation of the impact of inter-frame image motion on detection performance

Inter-frame additive walk generation: For the purpose of understanding the impact of image motion on detection performance, we add additional inter-frame image motion to the GPS/INS stabilised image sequence, and then run our baseline detection system over this degraded image sequence data.
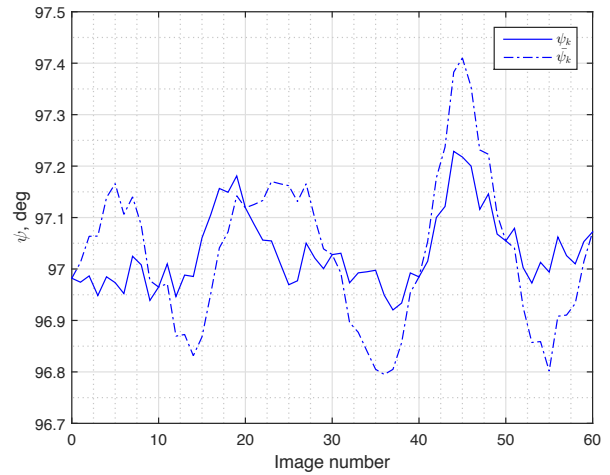

Fig. 8. Illustrative example of heading information corrupted caused by additive deterministic walk of size $D = 1$.

To simplify our analysis we simulated the additional image motion via an additive deterministic walk cycle of ten steps. Let D denote the size of the inter-frame motion in units of pixel, then the deterministic walk cycle (of amplitude $5D$) is described, for $k > 0$ by

$$\begin{aligned} \Delta\theta_k &= D(\mathrm{mod}(k+5,10)-5), \\ \Delta\psi_k &= D(\mathrm{mod}(k+5,10)-5). \end{aligned} \quad (3)$$

This additive walk can be used to generate modified attitude angles $\bar{\theta}_k, \bar{\psi}_k$ as follows:

$$\begin{aligned} \bar{\theta}_k &= \theta_k + R_\theta \Delta\theta_k \\ \bar{\psi}_k &= \psi_k + R_\psi \Delta\psi_k \end{aligned} \quad (4)$$

where θ_k, ψ_k are the GPS/INS solution for pitch and heading at time k, and R_θ, R_ψ are orthogonal angular resolutions of the sensor system in units of degree/pixel. Figure 8 shows an example of the GPS/INS ψ_k heading solution and modified heading angle $\bar{\psi}_k$ after the addition of a walk noise with $D = 1$ pixel.

An alternative stabilised image sequence (containing this additional uncompensated motion) can then be produced by using these modified attitude angles $\bar{\theta}_k, \bar{\psi}_k$ to stabilise the raw image sequence using the image sequence stabilisation process described earlier in Section III-A but with $\bar{\theta}_k$, $\bar{\psi}_k$ used in place of θ_k, ψ_k, respectively.

Performance in the presence of inter-frame additive walk: The 15 encounters were examined with the 3 threshold choices of: 0.45, 0.6 and 0.8. Figure 9 shows what proportion of encounters could successfully achieve detection with increasing additive walk size. This figure shows that with threshold $T_D = 0.45$ detection occurred in all datasets until $D = 0.6$, that there was significant reduction in performance for $D > 0.9$, but detection still occurred in some encounters for $D < 1.6$. Moreover, the figure shows that the detection system was less able to withstand additional inter-frame motion when detection threshold T_D was increased.
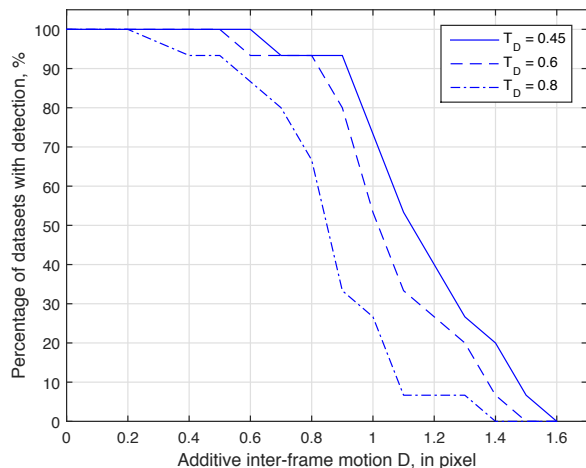
Fig. 9. The proportion of encounters with successful detection versus additive walk size. Performance reduces significantly for $D > 0.9$ and with increasing threshold T_D.

Fig. 10. Average detection distance versus additive deterministic walk size, averaged over 14 encounters[2]. Standard error bars are shown.

The encounter 3 experienced increased turbulence during flight, and exhibited increased residue inter-frame image motion following the GPS/INS image stabilisation such that detection did not occur for $D > 0.6$, and hence this encounter was removed from the next study of average detection distance versus D. The detection distance of the remaining 14 encounters for different D was examined with the 3 threshold choices of: 0.45, 0.6 and 0.8. Figure 10 shows the average our SAA system detection distance as a function of the size of additive walk. Only those data points at which detection was achieved in all 14 encounters are shown in this figure (thus explains why there are no data points for $D > 0.9$). This figure (unsurprisingly) shows that detection distance decreases with increasing threshold T_D and increasing size of additional additive walk D. This observation and Figure 9 suggests the setting threshold T_D as low as possible (whilst ensuring zero false alarm rate) achieves longer detection distances and greatest robustness to inter-frame motion. Alternatively, Figure 10 suggests that improving inter-frame stabilisation improves detection performance at a given threshold value.

Finally, we note that an inter-frame motion of $D = 0.9$ pixels added to the residue inter-frame motion of 1.1 pixels that was measured in Section IV-B illustrates that the basic detection system can tolerate inter-frame motion as great as 2 pixels with a detection threshold $T_D = 0.45$. This observation is consistent with previous reports about the amount of inter-frame motion that can be handled by Morphological-Hidden Markov model filter detection approaches (where this limit stems from the size of morphological structuring element, which allowed 2 pixels in this implementation), see [6]. The unreliable but occasional detection capability for $D > 0.9$ described by Figure 9 occurs because the Hidden Markov model filters in the baseline detection system have some ability to "coast" over occasional inter-frame motions beyond the 2 pixel allowance, whilst the apparent
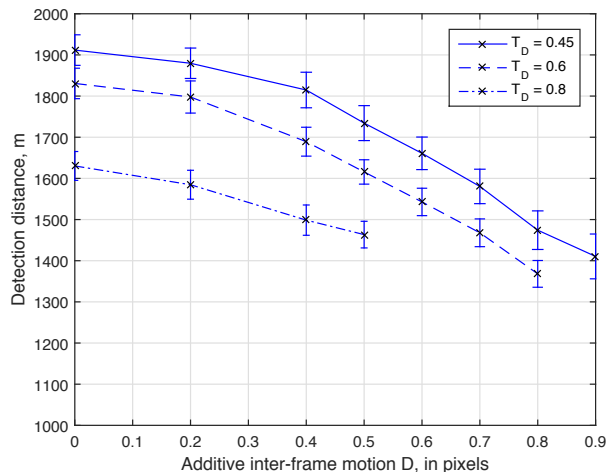
variation in inter-frame tolerance between encounters occurs because of variations in the residue inter-frame motion in each encounter.

Remark: Although not presented here, we also conducted studies where the additional additive motion was described by additive Gaussian noise, rather than the deterministic bounded walk described above. Analysis with additive Gaussian noise leads to observations similar to those presented here, however also demonstrates that the detection system has some ability to handle occasional inter-frame motion of a greater size (i.e. greater than 2 pixels). We are currently investigating methods for properly characterising the system capability when facing occasional inter-frame motion greater than 2 pixels.

D. Comparison of alternative techniques for image stabilisation

We considered the inter-frame stabilisation on the basis of the following attitude solutions:

- Aircraft GPS/INS attitude solution,
- Post-processed differential GPS/INS attitude solution,
- IMU-only attitude solution [27], and
- Image-based inter-frame stabilisation.

We begin with an illustrative comparison in Figure 11 which shows a comparison of the pitch attitude solution achieved by the GPS/INS, IMU-only stabilisation approaches and a post-processed (PP) attitude solution approach. The post-process solution was generated using differential GPS solution based on AUSPOS service[3] within the NovAtel Waypoint Inertial Explorer post-processing software. This differential GPS post-processed multipass NovAtel Waypoint Inertial Explorer solution cannot be implemented in real-time

---

[2]Encounter 3 was not included due to rough turbulence and excessive residue inter-frame image motion before any additional motion was even added.

[3]http://www.ga.gov.au/scientific-topics/positioning-navigation/geodesy/auspos
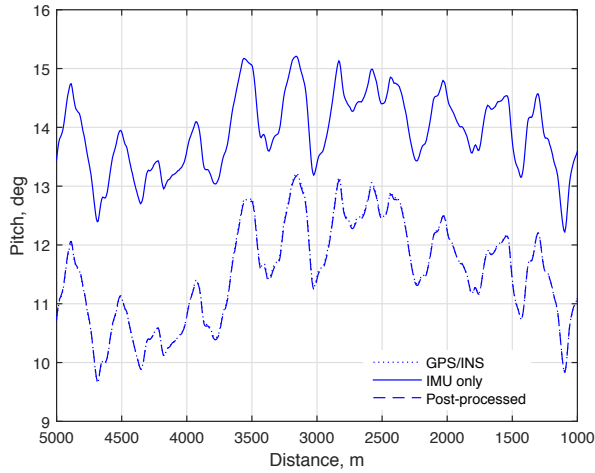
Fig. 11. Comparison of pitch attitude solution using GPS/INS stabilisation (dotted line), IMU only stabilisation (solid line) and Post-Processed (PP) solution (dashed line) during the 13th encounter. Note that the difference between pitch solutions arises due to the drift error that occurs in the pitch solution of the IMU only approach. However, for this detection system, it is the inter-frame motion not absolute angular accuracy that is important.
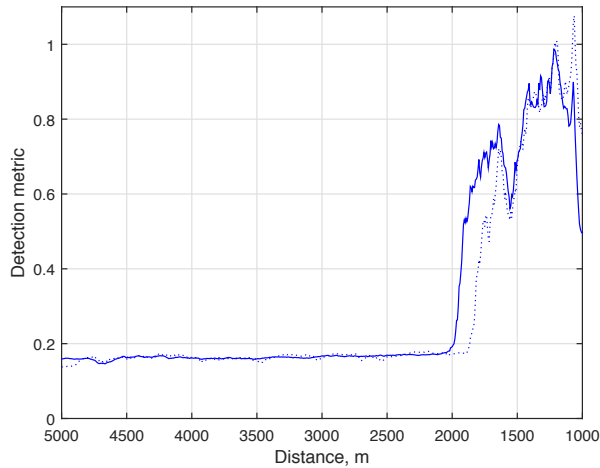

Fig. 12. Comparison of detection metric versus range using GPS/INS stabilisation (dotted line) and IMU-only stabilisation (solid line) in the 13th encounter. In this case, the IMU-only approach leads to an early detection alert (alerted at 1920 m compared to 1861 m, when $T_D = 0.45$).

but is included to illustrate the best performance that might be expected.

As expected, the offset in the IMU-only pitch attitude solution illustrates that the IMU-only stabilisation approach exhibits a drift in estimation accuracy over time (however, this offset may not matter because the performance of the detection approach is sensitive to inter-frame motion, rather than absolute accuracy). Figure 12 shows a detection metric comparison of the GPS/INS stabilisation approach with the IMU-only stabilisation approach. The performance of the two approaches is quite similar in this illustrative case, but the IMU-only approach leads to an earlier detection alert (alerted at 1920 m compared to 1861 m, when $T_D = 0.45$).

The candidate approaches were then more extensively compared on the basis of their detection distance performance on all encounters (unfortunately, insufficient IMU data was recorded in the 15th encounter to allow the IMU-only approach to be implemented). In this comparison, all detection systems use $T_D = 0.45$ (but we noted similar performance under other threshold choices). Table II shows the detection distance comparison of GPS/INS attitude solution approach, IMU-only attitude solution approach, PP attitude solution approach and the image-based stabilisation approach.

This table suggests roughly similar levels of detection distance performance when stabilised by either the GPS/INS or IMU-only approaches (although it is surprising that the IMU-only approach leads to similar mean detection distance, admittedly with higher variance, to the differential GPS post-processed stabilisation approach). Importantly, this study illustrates that the IMU-only approach is able to reduce inter-frame motion to an amount at least comparable to the GPS/INS approach, even though the absolute error in heading and pitch angle grows with time. Although not done here, the attitude drift might be further compensated using earth's magnetic sensor measurements (available in the Analog Devices ADIS-16488 IMU sensor). However, the benefits of the extra compensation are likely to be minor.

TABLE II

COMPARISON OF DETECTION DISTANCE FOR DIFFERENT STABILISATION APPROACHES. $T_D = 0.45$ (NO FALSE ALARM EVENTS). STANDARD DEVIATIONS SHOWN IN BRACKETS.

Encounter	GPS/INS, m	IMU, m	PP, m	Image, m
1	1792	1497	1732	1581
2	1869	2563	1969	1582
3	1573	1522	1599	1695
4	2113	2031	2121	1798
5	1810	1869	1903	1549
6	1801	2038	1801	1565
7	1980	2195	2180	1315
8	2031	1968	2013	1528
9	1976	2019	2286	1194
10	2184	1907	2184	1574
11	1946	1946	1939	1701
12	1861	1942	1942	1312
13	1776	1920	1828	1069
14	1857	1959	1900	1464
15	1715	n/a†	n/a†	1567
Average	1886	1955	1957	1502
	(156.9)	(256.1)	(189.3)	(195.3)

† Encounter 15 had insufficient IMU data recorded to allow either the IMU-only or the post-processed approach to be implemented.

The table also illustrates that, on average, an image-based inter-frame stabilisation approach achieved shorter detection distances than the other inertial sensor based approaches. It was noticed that the image-based approach was computationally slower and less accurate in environments with less distinct image features. Importantly, the image-based stabilisation approach out-performed the inertial based

approaches in encounter 3 (which involved significant flight turbulence and platform motion that was not inertially sensed accurately). Overall, considering the significantly reduced cost of the IMU-only approach, this study suggests that the IMU-only approach might be the preferred implementation approach in a real system.

V. Conclusions

This paper described the performance of a custom built image-based SAA system fitted to a ScanEagle UAV for testing purposes. This paper studied the impact of inter-frame motion on detection performance, and also evaluated the performance of several candidate stabilisation approaches. The investigation showed that the stabilisation requirement is related to a design choice within the detection algorithm. Significantly, this study also demonstrated that this inter-frame stabilisation requirement can be achieved using a much cheaper IMU-only stabilisation approach compared to the current expensive GPS/INS approach. Finally, this study suggested that inertial based approaches resulted in superior performance to image-based inter-frame stabilisation approaches.

Acknowledgment

References

[1] R. J. Kephart and M. S. Braasch, "Comparison of see-and-avoid performance in manned and remotely piloted aircraft," in Digital Avionics Systems Conference, 2008. DASC 2008. IEEE/AIAA 27th. IEEE, Oct. 2008, pp. 4.D.2-1-4.D.2-8.

[2] A. Finn and S. Franklin, "Acoustic sense & avoid for UAV's," in Intelligent Sensors, Sensor Networks and Information Processing (ISSNIP), 2011 Seventh International Conference on. IEEE, Dec. 2011, pp. 586-589.

[3] K. May and N. Krouglicof, "Moving target detection for sense and avoid using regional phase correlation," in IEEE International Conference on Robotics and Automation (ICRA), 2013 May 2013, pp. 4767-4772.

[4] D. Accardo, G. Fasano, L. Forlenza, A. Moccia, and A. Rispoli, "Flight test of a Radar-Based tracking system for UAS sense and avoid," IEEE Transactions on Aerospace and Electronic Systems, vol. 49, no. 2, pp. 1139-1160, Apr. 2013.

[5] J. N. Simon and M. S. Braasch, "Deriving sensible requirements for UAV sense-and-avoid systems," pp. 6.C.4-1-6.C.4-12, Oct. 2009.

[6] John Lai, Luis Mejias, Jason Ford, "Airborne Vision-based Collision-Detection System," Journal of Field Robotics, vol. 28(2), pp. 137-157, 2011.

[7] John Lai, Jason J. Ford, Luis Mejias, and Peter O'Shea, "Characterization of sky-region morphological-temporal airborne colision detection," Journal of Field Robotics 30(2), pp. 171-193, 2013.

[8] D. Dey, C. Geyer, S. Singh, and M. Digioia, "A cascaded method to detect aircraft in video imagery," The International Journal of Robotics Research, vol. 30, no. 12, pp. 1527-1540, Oct. 2011.

[9] A. Zarandy, Z. Nagy, B. Vanek, T. Zsedrovits, A. Kiss, and M. Nemeth, "A Five-Camera vision system for UAV visual attitude calculation and collision warning," in Computer Vision Systems, ser. Lecture Notes in Computer Science, M. Chen, B. Leibe, and B. Neumann, Eds. Springer Berlin Heidelberg, 2013, vol. 7963, pp. 11-20.

[10] Y. Barniv, "Dynamic programming solution for detecting dim moving targets," IEEE Transactions on Aerospace and Electronic Systems, vol. AES-21, no. 1, pp. 144-156, 1985.

[11] T. Gandhi, M.-T. Yang, R. Kasturi, O. I. Camps, L. D. Coraor, and J. Mccandless, "Performance characterization of the dynamic programming obstacle detection algorithm," IEEE Transactions on Image Processing, Vol. 15, no. 5, pp. 1202-1214, 2006.

[12] Lai, John S., Ford, Jason J., Mejias, Luis, Wainwright, Alexander Lloyd, O'Shea, Peter J., & Walker, Rodney A. "Field-of-view, detection range, and false alarm trade-offs in vision-based aircraft detection", In International Congress of the Aeronautical Sciences, 23-28 Sept. 2012, Brisbane, QLD.

[13] Lai, J., Ford, J. J., Mejias, L., O'Shea, P., & Walker, R., "See and avoid using on-board computer vision," in Sense and Avoid in UAS: Research and Applications, Chichester, Wiley, 2012, pp. 265-294.

[14] Xiang Yu and Youmin Zhang, "Sense and avoid technologies with applications to unmanned aircraft systems: Review and prospects", Progress in Aerospace Sciences, vol. 74, pp. 152-168, 2015.

[15] Mcfadyen, Aaron and Mejias, Luis (2016) "A Survey of autonomous vision-based See and Avoid for Unmanned Aircraft Systems". Progress in Aerospace Sciences, 80, pp. 1-17.

[16] A. Nussberger, H. Grabner, and L. Van Gool, "Aerial object tracking from an airborne platform," in IEEE International Conference on Unmanned Aircraft Systems (ICUAS), May 2014, pp. 1284-1293.

[17] R. W. Osborne, Y. Bar-Shalom, P. Willett, and G. Baker, "Design of an adaptive passive collision warning system for UAVs," Aerospace and Electronic Systems, IEEE Transactions on, vol. 47, no. 3, pp. 2169-2189, Jul. 2011

[18] Tirri, A. E., Fasano, G., Accardo, D., & Moccia, A. "Architectures and algorithms for non-cooperative sense and avoid". In IEEE Metrology for Aerospace (MetroAeroSpace), 2014, pp. 127-132, May 2014.

[19] A. Zarndy, M. Nemeth, Z. Nagy, A. Kiss, L. Santha, and T. Zsedrovits, "A real-time multi-camera vision system for UAV collision warning and navigation" In Journal of Real-Time Image Processing (2014), pp. 1-16

[20] Lai, John S., Ford, Jason J., O'Shea, Peter J., Walker, Rodney A., & Bosse, Michael "A Study of Morphological Pre-Processing Approaches for Track-Before-Detect Dim Target Detection." In Kim, Jonghyuk & Mahony, Robert (Eds.) 2008 Australasian Conference on Robotics & Automation, 3-5 December, 2008, Canberra.

[21] Fasano, G., Accardo, D., Tirri, A. E., Moccia, A., & De Lellis, E. "Morphological filtering and target tracking for vision-based UAS sense and avoid". In IEEE International Conference on Unmanned Aircraft Systems (ICUAS), 2014, pp. 430-440, May 2014.

[22] Tulpan, Dan, et al."Experimental evaluation of four feature detection methods for close range and distant airborne targets for Unmanned Aircraft Systems applications." In IEEE International Conference on Unmanned Aircraft Systems (ICUAS), 2014.

[23] Mejias, Luis, McNamara, Scott, Lai, John S., & Ford, Jason J. "Vision-based detection and tracking of aerial targets for UAV collision avoidance". In Proceedings of the 2010 IEEE/RSJ International Conference on Intelligent Robots and Systems (IROS), IEEE, Taipei International Convention Center, Taipei.

[24] Mejias, Luis, Lai, John S., Ford, Jason J., & O'Shea, Peter J. "Demonstration of closed-loop airborne sense-and-avoid using machine vision". IEEE Aerospace and Electronic Systems Magazine, 27(4), pp. 4-7.

[25] Yang, Xilin, Luis Mejias Alvarez, and Troy Bruggemann. "A 3D collision avoidance strategy for UAVs in a non-cooperative environment." Journal of Intelligent & Robotic Systems 70.1-4 (2013): 315-327.

[26] A. Mcfadyen, A. Durand-Petiteville and L. Mejias. "Decision strategies for automated visual collision avoidance." In IEEE International Conference on Unmanned Aircraft Systems (ICUAS), 2014.

[27] S. O. Madgwick, H. A. J.L. and R. Vaidyanathan, "Estimation of IMU and MARG orientation using a gradient descent algorithm.," IEEE International Conference on Rehabilitation Robotics : [proceedings], 2011.

[28] B. D. Lucas and T. Kanade, "An iterative image registration technique with an application to stereo vision. Proceedings of Imaging Understanding Workshop", pages 121–130, 1981.

[29] Gary R. Bradski and Adrian Kaehler. Learning opencv. computer vision with the opencv library. 2008.

[30] Simon Baker, Scharstein Daniel, J.P. Lewis, Stefan Roth, Michael J. Black, and Richard Szeliski, "A database and evaluation methodology for optical flow", Technical Report MSR-TR-2009-179, Microsoft Research, December 2009.

[31] M. Wilson, D. Ryan, D. Bratanov, A. Wainwright, J. Ford, L. Cork and M. Brouckaert, "Flight test and evaluation of a prototype sense and avoid system onboard a scaneagle unmanned aircraft". IEEE Aerospace and Electronic Systems Magazine, 2016, vol. 31(9), pp. 6-15.